Modeling Tumor Response after Combined Administration of Different Immune-Stimulatory Agents[S]

Zinnia P. Parra-Guillen, Pedro Berraondo, Benjamin Ribba, and Iñaki F. Trocóniz

Department of Pharmacy and Pharmaceutical Technology, School of Pharmacy, University of Navarra, Pamplona, Spain (Z.P.P.-G., I.F.T.); Division of Hepatology and Gene Therapy, Centre for Applied Medical Research, University of Navarra, Pamplona, Spain (P.B.); and INRIA Grenoble-Rhône-Alpes, Project-team NUMED, Saint Ismier, France (B.R.)

Received May 31, 2013; accepted July 10, 2013

ABSTRACT

The aims of this work were as follows: 1) to develop a semi-mechanistic pharmacodynamic model describing tumor shrinkage after administration of a previously developed antitumor vaccine (CyaA-E7) in combination with CpG (a TLR9 ligand) and/or cyclophosphamide (CTX), and 2) to assess the translational capability of the model to describe tumor effects of different immune-based treatments. Population approach with NONMEM version 7.2 was used to analyze the previously published data. These data were generated by injecting 5×10^5 tumor cells expressing human papillomavirus (HPV)-E7 proteins into C57BL/6 mice. Large and established tumors were treated with CpG and/or CTX administered alone or in combination with CyaA-E7. Applications of the model were assessed by comparing model-based simulations with preclinical and clinical outcomes obtained from literature. CpG effects were modeled: 1) as an amplification of the immune signal triggered by the vaccine and 2) by shortening the delayed response of the vaccine. CTX effects were included through a direct decrease of the tumor-induced inhibition of vaccine efficacy over time, along with a delayed induction of tumor cell death. A pharmacodynamic model, built based on plausible biologic mechanisms known for the coadjuvants, successfully characterized tumor response in all experimental scenarios. The model developed was satisfactory applied to reproduce clinical outcomes when CpG or CTX was used in combination with different vaccines. The results found after simulation exercise indicated that the contribution of the coadjuvants to the tumor response elicited by vaccines can be predicted for other immune-based treatments.

Introduction

A great effort is ongoing with the use of cancer vaccines since the identification of human cancer antigens that could be specifically recognized by the immune system (Dougan and Dranoff, 2009; Palucka and Banchereau, 2012). Cancer vaccines aim to induce tumor-specific T cells capable of reducing tumor mass and generating a permanent immune response via memory T cells. However, and despite promising initial results, poor clinical outcomes have been obtained mainly due to the low effector response triggered by vaccines in vivo, but also due to the appearance of tolerance mechanisms mediated by immunoregulatory cell populations such as regulatory T cells (Treg) that dampen the immune response

(Alpizar et al., 2011; Finn, 2012). A clear benefit has been observed both in preclinical and clinical settings when combination treatments targeting different aspects of the immune system at once are used (Copier et al., 2009; Beatty et al., 2011).

Different alternatives to increase the immunologic efficacy of immunotherapy have been discussed (Finn, 2003; Rosenberg et al., 2004; Copier et al., 2009). Among them, inhibition of the immunosuppressive mechanisms elicited by the tumor through depletion of the Treg cell population has shown promising results using drugs such as anti-CD25 antibodies or low doses of cyclophosphamide (CTX) (Onizuka et al., 1999 ; Ghiringhelli et al., 2007; Alfaro et al., 2011). Another approach widely studied has been the activation of antigen-presenting cells (especially dendritic cells) or other cells of the innate immune system to increase the number and/or avidity of the antigen-specific T cells with adjuvants such as Toll-like receptor (TLR) ligands or coadministration of different cytokines to potentiate and promote cell survival (Brody et al., 2010; Landrigan et al., 2011; Hong et al., 2012).

An example of these combination strategies is the work published by Berraondo et al. (2007), in which a potent vaccine obtained after the fusion of the adenylate cyclase of *Bordetella pertussis* (an enzyme able to target antigen to dendritic cells) to the human papillomavirus E7 protein (CyaA-E7) was used

ABBREVIATIONS: CTX, cyclophosphamide; CyaA-E7, vaccine obtained after the fusion of the adenylate cyclase of *Bordetella pertussis* to the human papillomavirus E7 protein; IL-12, interleukin 12; PK/PD, pharmacokinetic/pharmacodynamic; TLR, Toll-like receptor; Treg, regulatory T-cells; Ts, tumor size.

(Préville et al., 2005). However, a progressive loss of efficacy was observed when the vaccine was used to treat larger tumors in mice. In their work, the authors showed how combination regimens of the CyaA-E7 with different coadjuvant therapies such as CTX or CpG, a TLR9 ligand, could increase vaccine efficacy (Berraondo et al., 2007). Moreover, a percentage of cure (complete disappearance of tumor lesions) close to 90% was observed when the three drugs were simultaneously administered to treat large tumors, thus becoming an interesting treatment strategy to be tested in human patients.

Although recent examples have shown an agreement between xenograft-derived results with cytotoxic and targeted agents when using the proper quantitative framework and clinical response (Rocchetti et al., 2007; Wong et al., 2012), quantitative analysis applying population pharmacokinetic/pharmacodynamic principles is still scarce in the area of immunotherapy, especially in preclinical tumor models and, moreover, in combination dosing regimens (Gorelik et al., 2008; Choo et al., 2013).

A couple of modeling approaches have been proposed to study the interaction between coadministered drugs, assuming that both drugs induced a direct killing of tumor cells (Koch et al., 2009; Rocchetti et al., 2009). However, when dealing with immune system, more mechanistic models are required to better capture the complexity of the system and the effects triggered by the different therapies. In this regard, noteworthy models include the one proposed by Bunimovich-Mendrazitsky et al. (2011) to describe the interactions of immune and tumor cells after combined administration of bacillus Calmette-Guérin and interleukin 2 in superficial bladder cancer, or the one proposed by Harrold et al. (2012) including receptor occupancy and signal transduction dynamics to predict tumor growth profiles after administration of rituximab in combination with an apoptosis-inducing ligand or a cytotoxic agent.

A pharmacokinetic/pharmacodynamic (PK/PD) model to describe the antitumor response triggered by single immunotherapies has been previously developed and validated in our group (Parra-Guillen et al., 2013). The aim of the present work was to expand the mathematical modeling framework developed to incorporate the pharmacodynamic effects triggered by coadjuvants in immunotherapy, capturing the key biologic mechanisms implied in a simple but meaningful way. Moreover, we evaluated the translational impact of the semimechanistic PK/PD drug combination model by comparing model-based simulations with efficacy results derived from clinical trials extracted from literature (Höltl et al., 2005; Rynkiewicz et al., 2011; Walter et al., 2012).

Materials and Methods

Experimental Data and Studies Design

Data published by Berraondo et al. (2007) regarding combination therapy were used to build the PK/PD drug combination model. In brief, in their experiments, 5×10^5 TC-1 tumor cells expressing human papillomavirus E7 protein were injected into the shaved backs of 5-week-old female C57BL/6 mice and the efficacy of CTX (Sigma-Aldrich, St. Louis, MO) and/or CpG (CpG 1826: 5-TCCATGACGTTCCTGACGTT-3, synthesized by Proligo, Boulder, CO) in combination with CyaA-E7 vaccine was tested under different experimental settings (Fig. 1). CyaA-E7 and CpG were given intravenously, whereas CTX was administered intraperitoneally. CpG was complexed with the cationic

lipid N-[1-(2,3-dioleoyloxyl)propyl]-N,N,N-trimethylammoniummethyl sulfate (DOTAP; Roche, Indianapolis, IN) to protect it from degradation and to facilitate its uptake (Honda et al., 2005).

Bitherapy. A single 50-μg dose of CyaA-E7 on day 25 in combination with either a 30-μg dose of CpG on the same day or 2.5-mg dose of CTX on the previous day were given ($n = 12$ in both experiments). Two additional groups of mice receiving CpG ($n = 12$) or CTX ($n = 11$) in monotherapy with the same dosing schedule were also included.

Tritherapy. A single dose of CyaA-E7 (50 μg) on day 25 ($n = 18$), 30 ($n = 12$), or 40 ($n = 12$) after tumor cell inoculation, along with CpG (30 μg) on the same day, and CTX (2.5 mg) on the previous day were administered. A group receiving a combination of CpG on day 25 and CTX on day 24 ($n = 17$) at the same dosing level was also considered.

Tumor size measurements were reported as the average of two perpendicular diameters and mice with a tumor size higher than 20 mm were sacrificed according to the institutional guidelines for animal care.

### Mathematical Model and Data Analysis

Tumor size (Ts) measurements, including those values below the limit of quantification (BQL) of 2 mm and treated as censored information (Beal, 2001), were described simultaneously based on the population approach with the NONMEM version 7.2 (Beal et al., 2006) using the Laplacian numerical estimation method. Data were logarithmically transformed. Interanimal variability (IAV) in model parameters was modeled using an exponential model, and an additive error in the logarithmic domain of the transformed data was used to describe the residual variability.

Model development was partly data driven and partly based on the known mechanism of action of CTX and CpG. It was performed in two steps: 1) data after administration of CTX or CpG alone and in combination with CyaA-E7 vaccine were described first, 2) models developed for bitherapy data (and model parameter estimates) were joined together to describe the Ts effects after tritherapy by simulation without any further parameter re-estimation.

Brief Description of the Vaccine Model for Ts Effects. The model included the following main aspects: 1) linear tumor growth, 2) kinetic-pharmacodynamic (K-PD) model (Jacqmin et al., 2007) describing vaccine (VAC) kinetics and vaccine effects through two transit compartment (TRAN$_{VAC}$ and SVAC), being effects over Ts controlled by SVAC, 3) a regulatory compartment (REG) controlled by the tumor and able to inhibit vaccine efficacy, and 4) finally, the existence of a subpopulation of mice able to trigger only a temporal tumor response to describe the relapse observed in a small size of the studied population. Figure 2 presents the schematic and mathematical representation of the vaccine model previously developed (yellow section), including a table with the parameter estimates for both CyaA-E7 and interleukin 12 (IL-12) agents (Parra-Guillen et al., 2013).

The parameters characterizing the vaccine model are the following: λ is the zero order rate constant of tumor growth, k_1 represents the first-order rate constant controlling vaccine elimination and transit between compartments, k_2 is the first-order rate constant accounting for SVAC degradation (k_{2_pop1} for responders and k_{2_pop2} for nonresponders), k_3 is the vaccine efficacy second-order rate constant, and k_4 represents the first-order rate constant controlling the regulator compartment dynamics. P(1) corresponds to the percentage of responders mice within the studied population, REG$_{50}$ represents the amount in the regulator compartment needed to inhibit vaccine activity by a half, and γ the steepness of the k_3-versus-REG relationship. Estimated interanimal variability on λ and REG$_{50}$ for CyaA-E7 and IL-12, respectively, were also used.

Description of the Final Models Developed for Drug Combination. Similarly to the vaccine case, pharmacokinetic data were not available for either of the coadjuvants; therefore, exponential decay was assumed following kinetic-pharmacodynamic approach (Jacqmin et al., 2007) (eq. 1). Two transit compartments were introduced
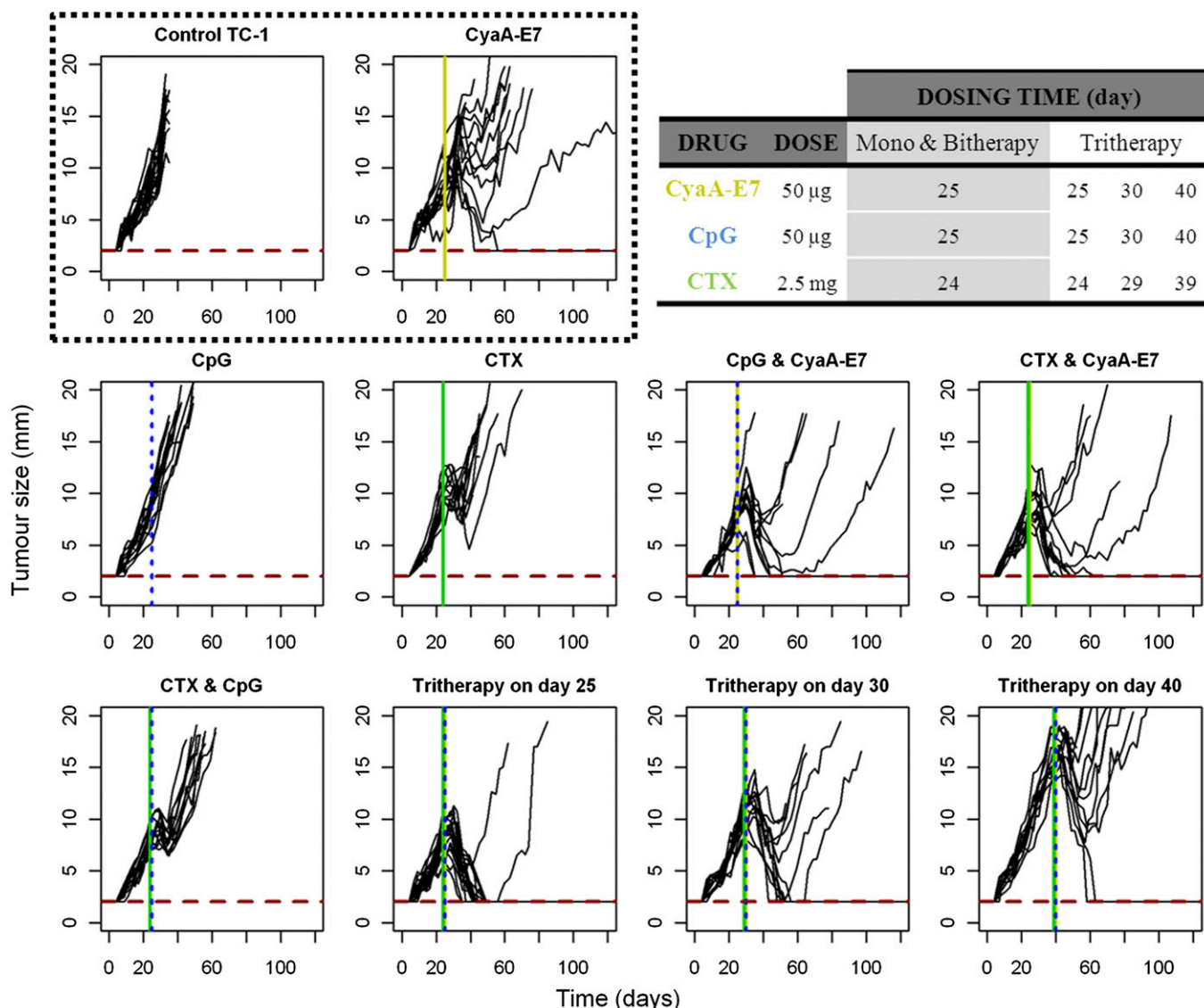
Fig. 1. Individual raw data profiles. C57BL/6 mice were injected with 5×10^5 TC-1 cells (n = 13–19 mice per group) on day 0. Individual mice profiles, computed as the mean of two perpendicular diameters, are shown after administration of a single dose of CyaA-E7 (yellow line), CpG (blue dashed line), or CTX (green line) alone, in two-two combination or after tritherapy administration (Berraondo et al., 2007). A table summarizing the drug doses used along with the day of dose administration has been included. Two millimeters was considered as the limit of quantification (red dashed line). Frame plots data belong to the monotherapy analysis previously published but are shown for comparison.

to account for the delayed response ($TRAN_D$ and S_D), where S_D is the compartment responsible of the effects over T_S (eqs. 2–3), D refers either to CTX or CpG, and k_D represents the first-order rate constant controlling coadjuvant drug elimination and transit between compartments.

$$\frac{dD}{dt} = -k_D \times D \tag{1}$$

$$\frac{dTRAN_D}{dt} = k_D \times D - k_D \times TRAN_D \tag{2}$$

$$\frac{dS_D}{dt} = k_D \times TRAN_D - k_D \times S_D \tag{3}$$

Using bitherapy data only, the following modifications accounting for CpG induced response were incorporated into the model developed for the CyaA-E7 effects: CpG both: 1) amplifies and 2) accelerates the immune response triggered by the vaccine (eqs. 4–6):

$$\frac{dVAC}{dt} = -k_1 \times VAC \times (1 + SLP_{CpG} \times S_{CpG}) \tag{4}$$

$$\frac{dTRAN_{VAC}}{dt} = k_1 \times (VAC\text{-}TRAN_{VAC}) \times (1 + SLP_{CpG} \times S_{CpG}) \tag{5}$$

$$\frac{dSVAC}{dt} = k_1 \times TRAN_{VAC} \times (1 + SLP_{CpG} \times S_{CpG}) - k_2 \times SVAC + k_5 \times S_{CpG} \times SVAC \tag{6}$$

where k_5 is second-order rate constant controlling SVAC amplification induced by CpG and SLP_{CpG} represents the linear effect triggered by CpG over the vaccine compartment dynamics.

Regarding CTX, its effects were incorporated into the model through a direct decrease of the synthesis process of REG compartment, thus diminishing the resistance phenomena, along with a delayed induction of tumor cell death (eqs. 7 and 8),
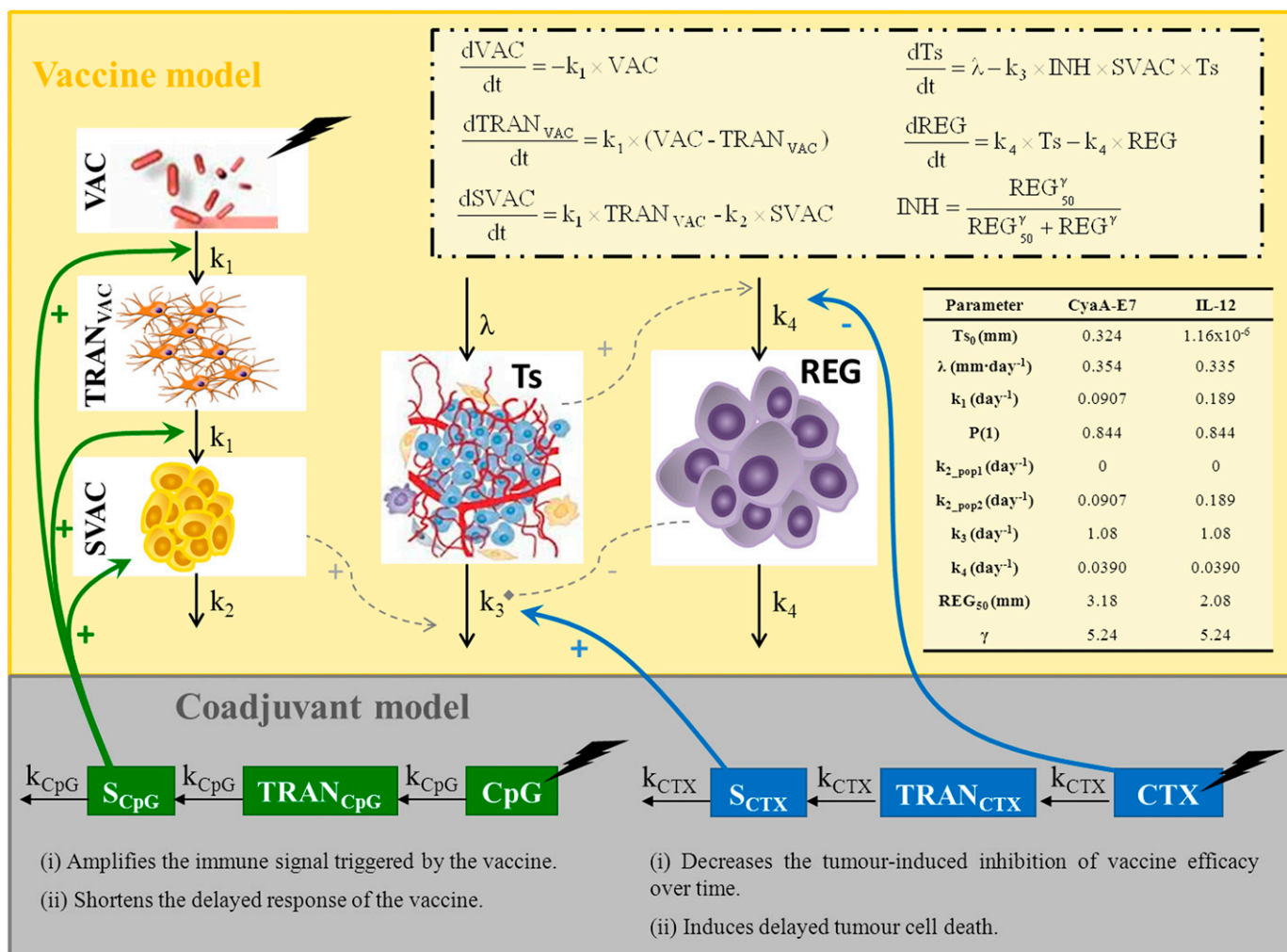
Fig. 2. Schematic representation of the combination therapy model. Previously developed vaccine model, equations, and parameter estimates for CyaA-E7 and IL-12 administration in monotherapy are shown (yellow area) (Parra-Guillen et al., 2013). After CpG administration and through a transit compartment ($TRAN_{CpG}$), the drug triggers a signal (S_{CpG}) able to increase transit between vaccine compartments and induce the proliferation of the vaccine signal (SVAC), which in turn will trigger tumor (Ts) death. On the other hand CTX is able to directly inhibit regulator compartment (REG) proliferation and generate, through a delay compartment ($TRAN_{CTX}$), a signal (S_{CTX}) able to induce tumor death. A description of the parameters can be found under *Materials and Methods*.

$$\frac{dTs}{dt} = \lambda - (k_3 \times SVAC + k_6 \times S_{CTX}) \times \frac{REG_{50}^{\gamma}}{REG_{50}^{\gamma} + REG^{\gamma}} \times Ts \quad (7)$$

$$\frac{dREG}{dt} = k_4 \times Ts \times (1 - SLP_{CTX} \times CTX) - k_4 \times REG \quad (8)$$

where k_6 is the CTX efficacy second-order rate constant and SLP_{CTX} represents the linear effect triggered by CTX over the REG compartment dynamics.

The initial conditions for all the compartments in the model were zero with the exception of Ts. At the time of drug administration, and given the absence of pharmacokinetic data, an arbitrary dose of value 1 was considered for VAC, CTX, and CpG. The combination model, mathematically represented by the set of ordinary differential eqs. 1–8, is depicted schematically in Fig. 2 (gray area).

Model Selection and Evaluation. Selection between models was based mainly on the goodness-of-fit plots and precision of parameter estimates obtained from the analysis of one thousand bootstrap datasets using the software Perl-speaks-NONMEM (Lindbom et al., 2005). In addition, the minimum value of the objective function (MOFV) value provided by NONMEM and approximately equal to $-2 \times \log$ (likelihood) (–2LL) was used (Beal et al.,

2006). Differences between two hierarchical (nested) models were compared with a χ^2 distribution in which a decrease of 6.63 points in –2LL was considered significant at the 1% level for one extra parameter in the model (Beal and Sheiner, 1982). Non-nested models were compared using the Akaike information criteria (AIC) (Ludden et al., 1994). The model with the lowest value of AIC, given the precision of model parameters, and an adequate description of the data was selected.

Internal model evaluation was graphically explored by simulating 1000 datasets with the same study design characteristics as the original one (Parra-Guillen et al., 2013). Simulated tumor size time-course, percentage of BQL over time, and probability of cure at the end of the study, including the 90% confidence interval, were plotted and compared with the raw data. Probability of cure was calculated as the ratio between the number of mice in which predicted tumor size was below the limit of quantification at the end of the study and the total number of mice in each group. External model validation was performed using the tritherapy data as it has been described above for internal model evaluation.

Preclinical Application of the Model. Data published by Medina-Echeverz et al. (2011) were used ($n = 12$). Briefly, 5×10^5 MC38 cells were subcutaneously injected to 5-week-old female C57BL/6

mice and 10 μg of a plasmid codifying for murine IL-12 administered by hydrodynamic injection on day 23 in combination with CTX on the previous day were given. Tumor size data were simulated using the same model structure developed for CyaA-E7, but with the specific set of parameters previously estimated for IL-12 immunotherapy (summarized in Fig. 2) (Parra-Guillen et al., 2013), coupled with the CTX model here developed. Simulations were graphically inspected and compared versus raw data as described in model evaluation section.

Extrapolation to Clinical Setting. A literature search in Pubmed was performed to find clinical trials where immunotherapeutic agents had been administered alone and in combination with CpG and/or CTX. The following MeSH terms were used during the searches "clinical trial," "immunotherapy," "vaccine," "cyclophosphamide," and "CpG oligonucleotides." Three articles were selected in which the immunotherapeutic agent under study had been given alone and in combination with CTX or CpG:

1. Höltl et al. (2005): Safety and efficacy of allogenic dendritic cells with and without CTX were evaluated in a phase I/II study. The treatment consisted in three vaccinations in monthly intervals. If applicable, a dose of 300 mg/m^2 CTX infused during 2 hours was given on days 3 and 4 prior each vaccination. Clinical outcome was reported as mixed response (MR), stable disease (SD), or progression disease (PD).
2. Rynkiewicz et al. (2011): CpG7909 safety and properties as coadjuvant were evaluated in combination with BioThrax (Anthrax Vaccine Adsorbed) in healthy volunteers. Intramuscular administrations of the vaccine mixed with 1 mg of CpG, if applicable, on days 0, 14, and 28 were performed. Clinical response was evaluated as percentage of subjects reaching a threshold for seropositivity (5 μg/ml) when measuring antiprotective antigen (main vaccine antigen) antibodies.
3. Walter et al. (2012): IMA901 vaccine for the treatment of renal cell cancer in a phase II study was studied in patients. Seven intradermal vaccine administrations in the first 5 weeks followed by ten further vaccinations at 3-week intervals for 30 weeks were given. One single infusion of CTX (300 mg/m^2) 3 days before first vaccine administration was given if applicable. Clinical response was assessed as partial response (PR), SD, and PD according to the response evaluation criteria in solid tumors (RECIST) criteria v1.0.

The contribution of CpG or CTX effects to the vaccine response in the three different studies was calculated as the increment in the clinical probability of response (SD + PR) obtained when coadjuvant therapies were incorporated. Then, the calculated contribution in the different clinical trials was directly compared with the increment on the probability of cure predicted by the model in mice. This increment in mice was calculated using the median probability of cure estimated using 1000 simulated studies where CyaA-E7 vaccine was administered on day 25 (dosing protocol achieving a probability of cure comparable to the clinical response reported) in combination with CpG (day 25) or CTX (day 24) and compared with the probability of cure induced by CyaA-E7 administration in monotherapy.

Results

Brief Description of the Data

When CpG was administered alone, almost no effect was recognized (Fig. 1); however, when combined with the vaccine, an efficacy improvement was observed (percentage of cured mice 50 versus 14% when vaccine administered alone) suggesting that CpG is able to improve vaccine response.

Regarding CTX, a certain effect of the drug in monotherapy was observed (Fig. 1), although insufficient to cure any of the treated mice. Similarly to the previous coadjuvant, when CTX was administered in combination with CyaA-E7, an increased percentage of cure was detected (58 vs. 14%).

When CTX and CpG were given in combination, the resulting Ts profiles were found to be similar to those seen in the CTX control group.

Models for Drug Combinations

The model described by eqs. 1–8 and represented in Fig. 2 provided adequate precision for parameter estimates (see Table 1) and showed good performance in the individual (Fig. 3A) and in the population Ts profiles after bitherapy (both above and below the limit of quantification data) (Fig. 4). Moreover, the model described very well the results expressed as a probability of cure (Fig. 3B). During model development, a different number of transit compartments, likewise different CpG or CTX effects over other model components, or nonlinear models (e.g., E_{max}-type models) were explored and fitted to the data without achieving better description of the data. Supplemental Table 1 lists a summary of the main models fitted to the data. Inclusion of interanimal variability terms in the coadjuvant-related parameters was not supported by the data. In fact, visual predictive checks shown in Fig. 4 suggest that the variability in the tumor size observations is well captured by the model.

Merging together the selected models accounting for the combination of CyaA-E7 with CpG or CTX and simulating based on the corresponding final parameter estimates (Table 1), a satisfactory prediction of the Ts profiles after administration of tritherapy was obtained (Figs. 3 and 4) confirming the robustness of the combination model.

The effect of mono-, bi-, or tritherapy over Ts and REG compartments in both mouse populations (responders and nonresponders) is explored in Fig. 5, assuming that the CyaA-E7 is administered at day 25 where tumor shows resistance. Both effects of CpG were related to the vaccine compartments, and therefore, in the absence of vaccine, no drug-related effects were observed. When vaccine was coadministered with CpG, the area under the curve of the signal vaccine was doubled and peaked approximately 7 days

TABLE 1
Parameters of the mathematical model developed

| Parameter	CpG		CTX	
	Mean Value (CV%)	[2.5th–97.5th]	Mean Value (CV%)	[2.5th–97.5th]
k_D (day^{-1})	0.268 (5)	[0.0533–0.420]	0.302 (21.3)	[0.233–0.483]
SLP_D (au^{-1})	9.01 (8.1)	[3.52–62.3]	2.30 (40.7)	[1.25–4.48]
k_5 (au^{-1} · day^{-1})	0.478 (14.7)	[0.0847–1.65]	—	
k_6 (au^{-1} · day^{-1})	—		0.189 (45.6)	[0.0606–0.283]
Residual error [Log (mm)]	0.166 (6.7)	[0.144–0.189]	0.153 (4.7)	[0.133–0.166]
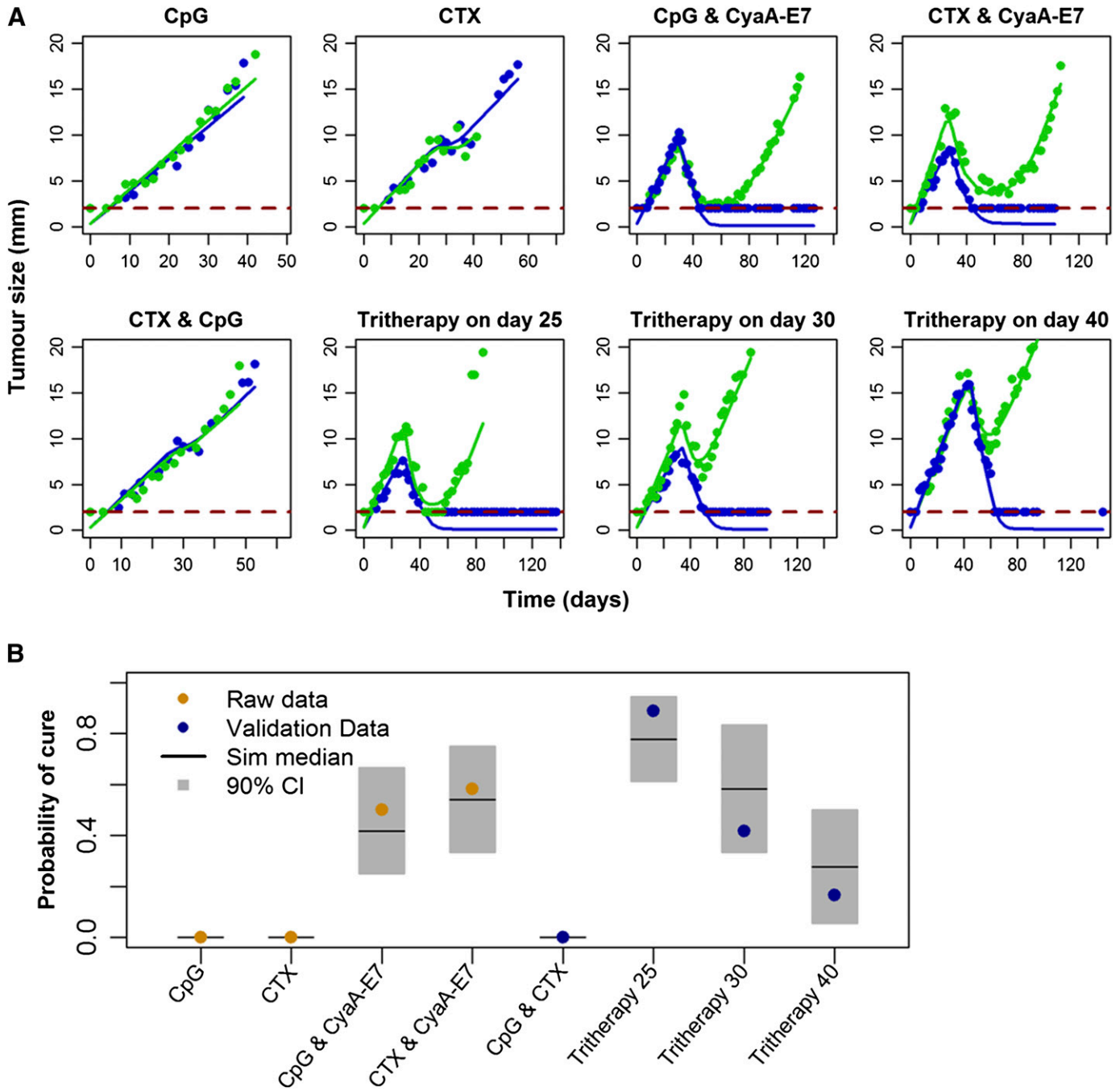
Fig. 3. Evaluation of model performance. (A) Tumor size observations (points) and individual model predictions (lines) of two illustrative mice per dosing group (obtained using the MAXEVAL=0 option in NONMEM) are presented using a different color for each mouse. 2 mm was considered as the limit of quantification (dashed line). (B) Probability of cure calculated over 1000 simulated studies is presented and compared with real data. Gray shadow represents 90% prediction interval of the simulated data and points represents the raw probability of cure for the studies used during model development (orange) and for the validation studies (blue).

earlier. Although CpG did not have a direct effect over REG compartment, an initial decrease on tumor size induced by the faster and more potent vaccine response triggered by CpG translated into a decrease in REG compartment levels, and thus a reduction in the inhibitory REG effect over k_3. Although a small inhibitory reduction was quantified (from 99 to 97% on day 42 when SVAC concentrations peaked) it proved to be enough to allow for tumor shrinkage in the responders group.

Regarding CTX, a maximum effect was achieved 3.5 days after administration with a 27% reduction on REG compartment, enough to decrease the inhibitory effect triggered by REG over k_3 by 85%, and thus allowing vaccine to be effective again. In the nonresponder group, tumor regrowth was observed once the CTX was cleared from the body, estimating a delay of disease progression of 9 days.

Although full tumor size shrinkage was observed with both bitherapies or tritherapy in those mice responding to the
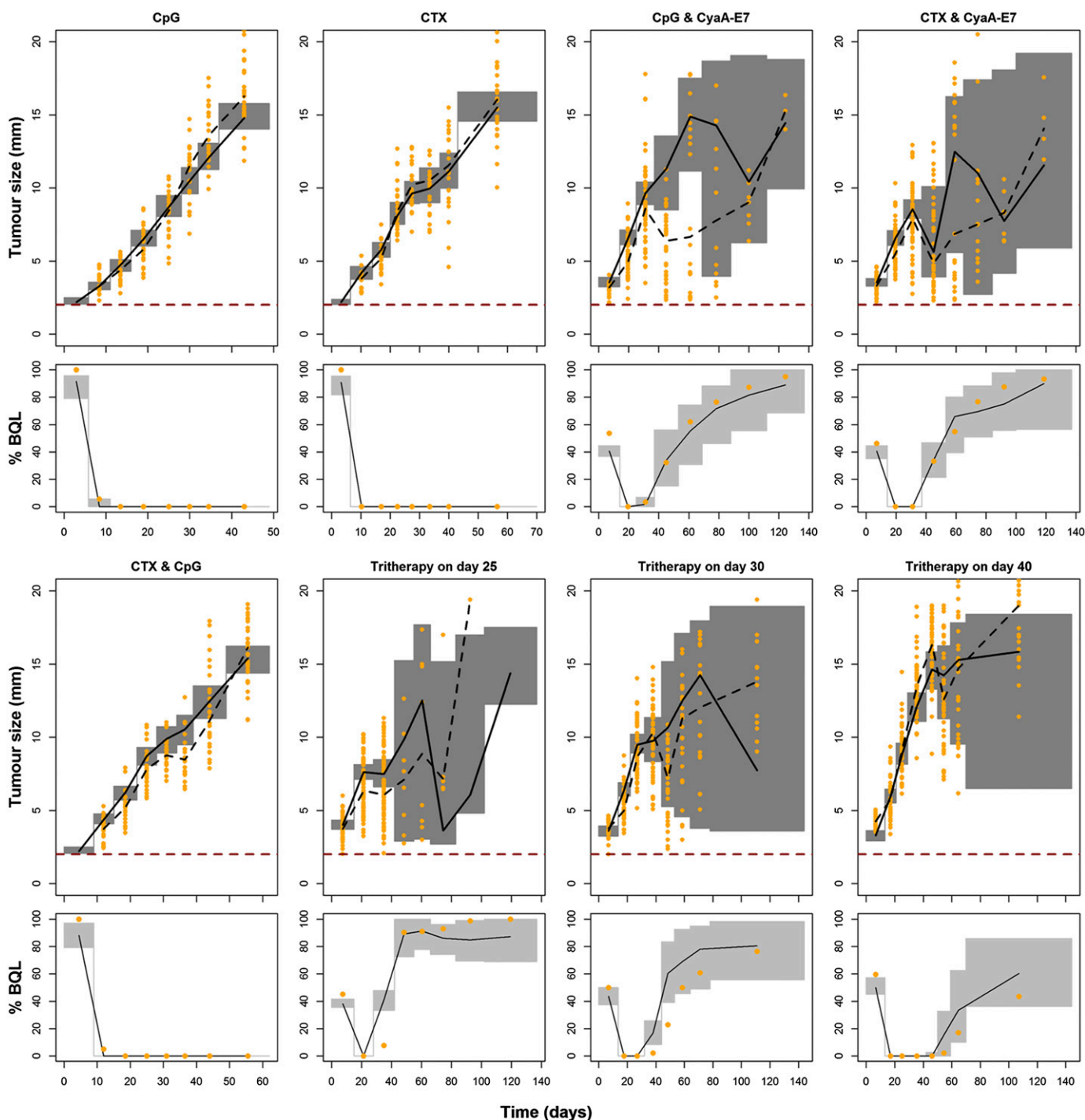
Fig. 4. Visual and numerical predictive check to evaluate final model performance at population level. Simulated tumor size measurements above the limit of quantification (upper panels) and percentage of data below the limit of quantification (lower panel) vs. raw data (points) are plotted over time for CyaA-E7 bitherapy and tritherapy studies. Gray areas in the upper panels represent the 90% prediction interval of the simulated median. Gray areas in the lower panels represent the 90% prediction interval of the simulated percentage of data below the limit of quantification. Solid and dashed black lines are the simulated and raw median respectively. Two millimeters was considered as the limit of quantification (red dashed line).

treatment (Fig. 5), higher percentage of cure (when variability in the parameters is taking into account) (Fig. 3B) and faster tumor shrinkage were predicted with tritherapy, reaching maximum tumor shrinkage 8 days after treatment (vs. 20 or 42 days with CTX or CpG, respectively). Similarly, in the nonresponders group, a prolonged time to disease progression was observed with tritherapy (26 days) compared with both bitherapies (15 for CpG and 18 for CTX days). This results show the benefit of combining therapies with different mechanism of action in the treatment of cancer.

Application of the Model

Simulation studies were undertaken to assess the capacity of the model to predict tumor response to different
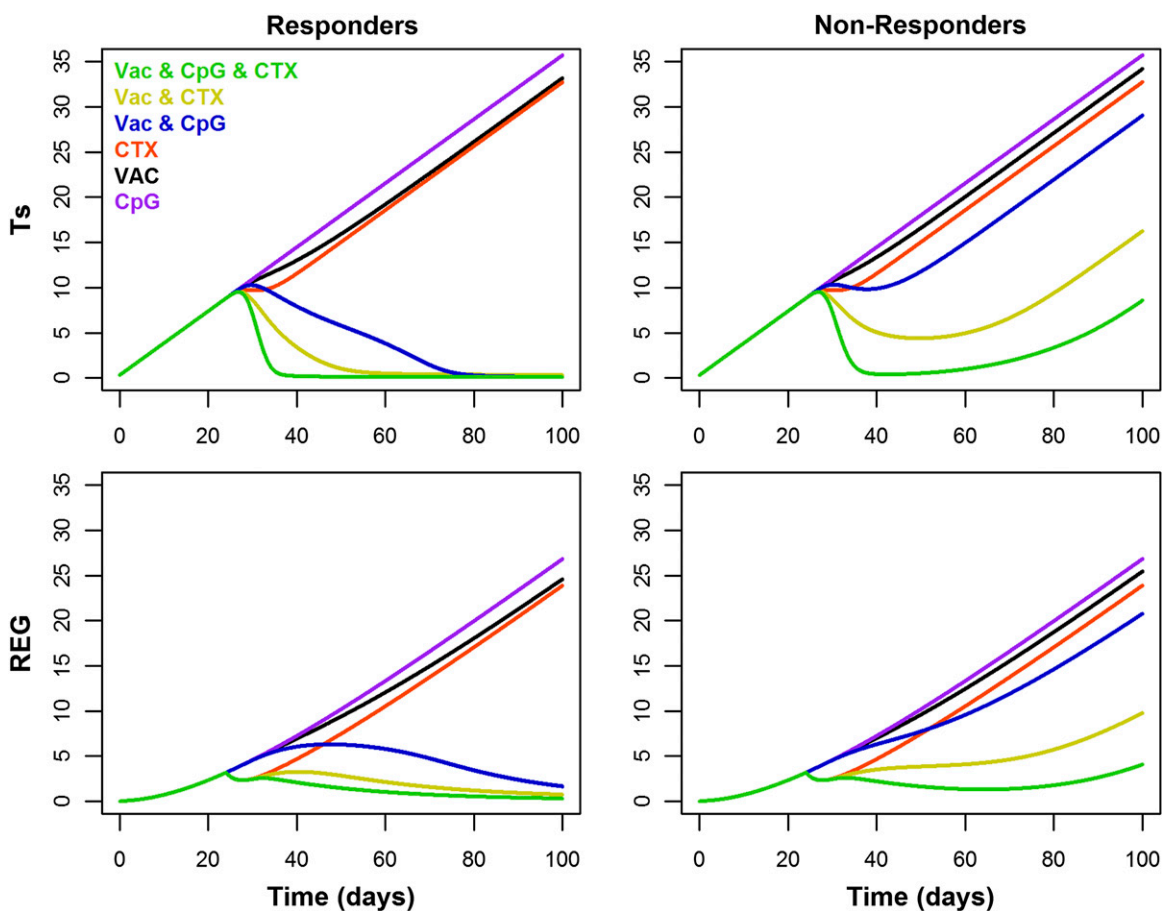
Fig. 5. Mean model performance. Tumor size (Ts) and regulator compartment (REG) profiles over time are presented for both mouse populations, responders (left) and nonresponders (right), after administration of 50 μg of CyaA-E7 on day 25, 30 μg of CpG-B on day 25, and/or 2.5 mg of CTX on day 24, alone or in combination.

immunotherapeutic agents when administered in combination with either CpG or CTX using literature data.

Preclinical. Figure 6 depicts the model performance at the individual and population level for IL-12. The results showed that the combination model developed can be applied to describe the time-course of tumor size in experiments performed to assess the response of different immune-therapeutic agents such as IL-12 when drug and tumor cell line–specific parameters are considered.

Extrapolation to Clinical Setting. Simulation results obtained from the model developed from preclinical data predicted an increase in the probability of cure of 0.27 [0.067–0.47] and of 0.33 [0.20–0.60] for CpG and CTX, respectively, with respect to monotherapy administration. Values similar to the 0.44 reported by Rynkiewicz et al. (2011) for CpG or the 0.17 and 0.25 reported by Walter et al. (2012), and Höltl et al. (2005), respectively, for CTX.

In addition, a 20% reduction on the number of Treg cells was found 3 days after treatment with CTX (Walter et al., 2012), a value comparable to the 27% that is predicted by our model assuming only one dose administration 24 hours prior to vaccine administration, indicating the potential role of the model in the optimization of future clinical trials.

Discussion

Over the past 30 years, vaccines have risen as an interesting approach in the treatment and prevention of cancer for a wide

range of tumors. However, it is unlikely that a potent and prolonged immune response can be obtained with monotherapy, as has been the case of chemotherapy.

Vaccine administration in combination with different coadjuvants to potentiate the triggered immune response or to inhibit the immunosuppressive mechanism developed by the tumor have proven to increase preclinical and clinical efficacy achieved in immunotherapy (Ghiringhelli et al., 2007; Alfaro et al., 2011; Mkrtichyan et al., 2011; Ge et al., 2012; Hong et al., 2012).

Evaluation of a wide range of drugs is a fundamental step in early drug development to assess synergistic, additive, or antagonistic interaction. PK/PD models provide a useful framework to assist in the evaluation and development of optimal therapeutic regimens in combination strategies (Rocchetti et al., 2009; Harrold et al., 2012).

In this article, we have expanded a previous semimechanistic model (Parra-Guillen et al., 2013) developed to characterize tumor growth dynamics after administration of an antitumor vaccine (CyaA-E7). The model was expanded to account for the pharmacodynamic effects triggered by CpG and CTX, two commonly used coadjuvants in immunotherapeutic regimens.

CpG is a TLR9 receptor ligand known to induce activation and maturation of antigen-presenting cells such as dendritic cells, increasing the number of antigen-specific T cells when coadministered with peptide vaccines (Speiser et al., 2005; Krieg, 2008). In addition, a faster response to peptide
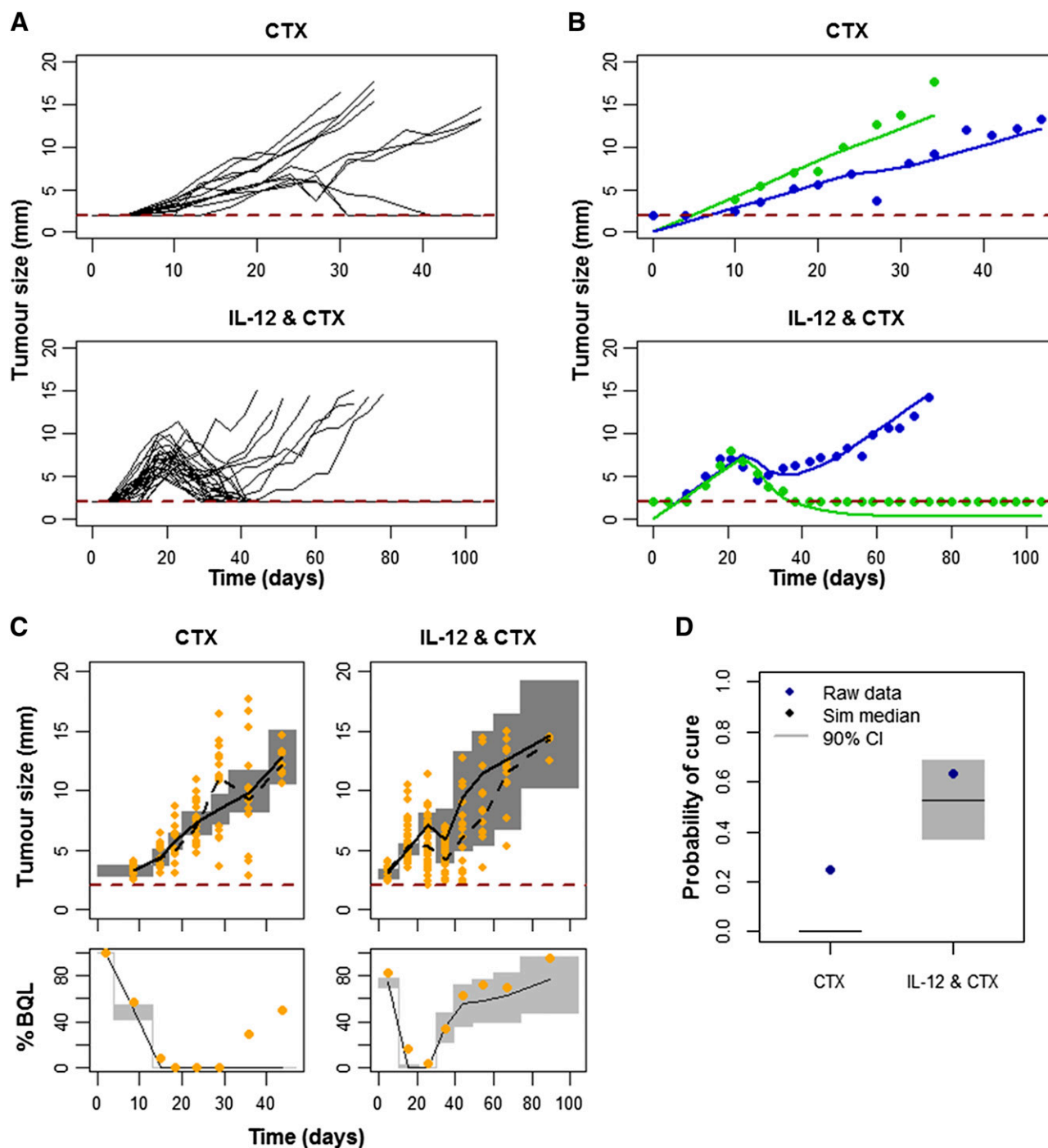
Fig. 6. External validation of the combination model using IL-12 experimental data. (A) C57BL/6 mice were injected with 5×10^5 MC38 cells on day 0. Individual mice profiles, computed as the mean of two perpendicular diameters, are shown after administration 2.5 mg of CTX on day 22 alone or in combination with 10 μg of a plasmid codifying for murine IL-12 administered by hydrodynamic injection on day 23. (B) Tumor size observations (points) vs. individual model predictions (solid lines obtained with MAXEVAL=0 option in NONMEM) of two mice per IL-12 dosing group. (C) Simulated tumor size measurements above the limit of quantification (upper panels) and percentage of data below the limit of quantification (lower panel) vs. raw data (points) are plotted over time for CTX administered alone or in combination with IL-12. Gray areas in the upper panels represent the 90% prediction interval of the simulated median. Gray areas in the lower panels represent the 90% prediction interval of the simulated percentage of data below the limit of quantification. Solid and dashed black lines are the simulated and raw median respectively. (D) Probability of cure calculated over 1000 simulated studies is presented and compared with real data. Gray shadow represents 90% prediction interval of the simulated data and points represents the raw probability of cure for the IL-12 studies. Two millimeters was considered as the limit of quantification (red dashed line).

administration, either measured as titer of antibodies (Ellis et al., 2010; Rynkiewicz et al., 2011) or as number of specific T cells (Speiser et al., 2005), has also been reported in protocols where CpG was coadministered. Regarding CTX,

administration of low doses has been described to deplete Treg cells by inhibiting their proliferation, and thus enhance tumor response (Lutsiak et al., 2005; Walter et al., 2012). Retaining a simplified representation of the biologic system,

our model has mechanistically incorporated the known pharmacology of the two coadjuvants, providing a successful description of the data comparable to other published results, which reported a decrease of around 20% 3 days after CTX administration (Walter et al., 2012) with a maximum effect reached 4 days after treatments and a recovery around day 11 (Mkrtichyan et al., 2011).

During the model-building process it was found that the incorporation of an extra effect of CTX represented as direct tumor shrinkage resulted in a significant fit improvement (Supplemental Table 1). Given the low doses used and the absence of CTX effect when nude mice were used [see supplementary figure in Berraondo et al. (2007)], this unexpected result suggests that CTX might also trigger other immune mechanisms represented by the parameter k_6 in the model.

It is worth noting that excellent predictions during tritherapy treatment were obtained simulating from the models developed with data from bitherapy without the need of further model refinements. A similar type of exercise has also been shown recently by Harrold et al. (2012).

The final developed model successfully described the data from CyaA-E7 and IL-12, both at the individual and the population levels, although some discrepancies were found for the IL-12 case given the presence of a few mice that did respond to CTX administration alone in contrast to what was observed for CyaA-E7.

Despite successful model performance to describe the data, a couple of model limitations have to be recognized. Lack of pharmacokinetic data or pharmacodynamic information at different dose levels or dosing regimens constitutes an important model limitation, since a proper link between drug concentration and effect cannot be established. Consequently, tumor size predictions under unexplored dosing regimens scenarios should be performed with great caution, and further experimental data will be needed to prove their validity. In addition, given the existing model complexity and data availability, interindividual variability in those parameters related to the coadjuvant therapy could not be incorporated into the model.

Given the minimum model developed to describe the system, parameter estimates do not reflect a unique physiologic process but a mixture of them (e.g., vaccine transit compartments reflect vaccine elimination and the different immune processes triggered after antigen presentation that ultimately lead to the proliferation of effector cells). Therefore, a direct interspecies scale is not feasible using classic allometric and/or species specific parameters.

Nevertheless, and regardless of previously mentioned drawbacks, the model was able to describe well and in a simplified manner the main mechanisms implied in the biologic responses triggered by both coadjuvants. Furthermore, the model was able to anticipate the clinical impact of adding CTX, or CpG coadjuvants to different immunotherapeutic agents using literature data, underscoring model robustness and translational capability to different clinical scenarios, although tumor size information would have been desirable to properly characterize the effect of the vaccines in monotherapy.

In summary, a semimechanistic model to account for the pharmacodynamic effects of two widely used coadjuvants in immunotherapy, CTX and CpG, in combination with different immunotherapeutic drugs has been proposed and validated under different experimental conditions. Moreover, the model was directly extrapolated to describe clinical outcomes, regarded as the percentage of individuals that would respond to the treatment, confirming model robustness and applicability to drug development.

References

Alfaro C, Perez-Gracia JL, Suarez N, Rodriguez J, Fernandez de Sanmamed M, Sangro B, Martin-Algarra S, Calvo A, Redrado M, and Agliano A, et al. (2011) Pilot clinical trial of type 1 dendritic cells loaded with autologous tumor lysates combined with GM-CSF, pegylated IFN, and cyclophosphamide for metastatic cancer patients. *J Immunol* **187**:6130–6142.

Alpizar YA, Chain B, Collins MK, Greenwood J, Katz D, Stauss HJ, and Mitchison NA (2011) Ten years of progress in vaccination against cancer: the need to counteract cancer evasion by dual targeting in future therapies. *Cancer Immunol Immunother* **60**:1127–1135.

Beal SL and Sheiner LB (1982) Estimating population kinetics. *Crit Rev Biomed Eng* **8**:195–222.

Beal SL (2001) Ways to fit a PK model with some data below the quantification limit. *J Pharmacokinet Pharmacodyn* **28**:481–504.

Beal S, Sheiner L, Boeckmann A (2006) NONMEM users guide [1989–2006].

Beatty PL, Cascio S, and Lutz E (2011) Tumor immunology: basic and clinical advances. *Cancer Res* **71**:4338–4343.

Berraondo P, Nouzé C, Préville X, Ladant D, and Leclerc C (2007) Eradication of large tumors in mice by a tritherapy targeting the innate, adaptive, and regulatory components of the immune system. *Cancer Res* **67**:8847–8855.

Brody JD, Ai WZ, Czerwinski DK, Torchia JA, Levy M, Advani RH, Kim YH, Hoppe RT, Knox SJ, and Shin LK, et al. (2010) In situ vaccination with a TLR9 agonist induces systemic lymphoma regression: a phase I/II study. *J Clin Oncol* **28**:4324–4332.

Bunimovich-Mendrazitsky S, Claude Gluckman J, and Chaskalovic J (2011) A mathematical model of combined *bacillus Calmette-Guerin* (BCG) and interleukin (IL)-2 immunotherapy of superficial bladder cancer. *J Theor Biol* **277**:27–40.

Choo EF, Ng CM, Berry L, Belvin M, Lewin-Koh N, Merchant M, and Salphati L (2013) PK-PD modeling of combination efficacy effect from administration of the MEK inhibitor GDC-0973 and PI3K inhibitor GDC-0941 in A2058 xenografts. *Cancer Chemother Pharmacol* **71**:133–143.

Copier J, Dalgleish AG, Britten CM, Finke LH, Gaudernack G, Gnjatic S, Kallen K, Kiessling R, Schuessler-Lenz M, and Singh H, et al. (2009) Improving the efficacy of cancer immunotherapy. *Eur J Cancer* **45**:1424–1431.

Dougan M and Dranoff G (2009) Immune therapy for cancer. *Annu Rev Immunol* **27**:83–117.

Ellis RD, Martin LB, Shaffer D, Long CA, Miura K, Fay MP, Narum DL, Zhu D, Mullen GE, and Mahanty S, et al. (2010) Phase 1 trial of the Plasmodium falciparum blood stage vaccine MSP1(42)-C1/Alhydrogel with and without CPG 7909 in malaria naïve adults. *PLoS ONE* **5**:e8787.

Finn OJ (2003) Cancer vaccines: between the idea and the reality. *Nat Rev Immunol* **3**:630–641.

Finn OJ (2012) Immuno-oncology: understanding the function and dysfunction of the immune system in cancer. *Ann Oncol* 23 (suppl 8):viii6-9.

Ge Y, Domschke C, Stoiber N, Schott S, Heil J, Rom J, Blumenstein M, Thum J, Sohn C, and Schneeweiss A, et al. (2012) Metronomic cyclophosphamide treatment in metastasized breast cancer patients: immunological effects and clinical outcome. *Cancer Immunol Immunother* **61**:353–362.

Ghiringhelli F, Menard C, Puig PE, Ladoire S, Roux S, Martin F, Solary E, Le Cesne A, Zitvogel L, and Chauffert B (2007) Metronomic cyclophosphamide regimen selectively depletes CD4+CD25+ regulatory T cells and restores T and NK effector functions in end stage cancer patients. *Cancer Immunol Immunother* **56**:641–648.

Gorelik B, Ziv I, Shohat R, Wick M, Hankins WD, Sidransky D, and Agur Z (2008) Efficacy of weekly docetaxel and bevacizumab in mesenchymal chondrosarcoma: a new theranostic method combining xenografted biopsies with a mathematical model. *Cancer Res* **68**:9033–9040.

Harrold JM, Straubinger RM, and Mager DE (2012) Combinatorial chemotherapeutic efficacy in non-Hodgkin lymphoma can be predicted by a signaling model of CD20 pharmacodynamics. *Cancer Res* **72**:1632–1641.

Höltl L, Ramoner R, Zelle-Rieser C, Gander H, Putz T, Papesh C, Nussbaumer W, Falkensammer C, Bartsch G, and Thurner M (2005) Allogeneic dendritic cell vaccination against metastatic renal cell carcinoma with or without cyclophosphamide. *Cancer Immunol Immunother* **54**:663–670.

Honda K, Ohba Y, Yanai H, Negishi H, Mizutani T, Takaoka A, Taya C, and Taniguchi T (2005) Spatiotemporal regulation of MyD88-IRF-7 signalling for robust type-I interferon induction. *Nature* **434**:1035–1040.

Hong S, Qian J, Li H, Yang J, Lu Y, Zheng Y, and Yi Q (2012) CpG or IFN-α are more potent adjuvants than GM-CSF to promote anti-tumor immunity following idiotype vaccine in multiple myeloma. *Cancer Immunol Immunother* **61**:561–571.

Jacqmin P, Snoeck E, van Schaick EA, Gieschke R, Pillai P, Steimer JL, and Girard P (2007) Modelling response time profiles in the absence of drug concentrations:

definition and performance evaluation of the K-PD model. *J Pharmacokinet Pharmacodyn* **34**:57–85.

Koch G, Walz A, Lahu G, and Schropp J (2009) Modeling of tumor growth and anti-cancer effects of combination therapy. *J Pharmacokinet Pharmacodyn* **36**:179–197.

Krieg AM (2008) Toll-like receptor 9 (TLR9) agonists in the treatment of cancer. *Oncogene* **27**:161–167.

Landrigan A, Wong MT, and Utz PJ (2011) CpG and non-CpG oligodeoxynucleotides directly costimulate mouse and human CD4+ T cells through a TLR9- and MyD88-independent mechanism. *J Immunol* **187**:3033–3043.

Lindbom L, Pihlgren P, and Jonsson EN (2005) PsN-Toolkit—a collection of computer intensive statistical methods for non-linear mixed effect modeling using NONMEM. *Comput Methods Programs Biomed* **79**:241–257.

Ludden TM, Beal SL, and Sheiner LB (1994) Comparison of the Akaike Information Criterion, the Schwarz criterion and the F test as guides to model selection. *J Pharmacokinet Biopharm* **22**:431–445.

Lutsiak ME, Semnani RT, De Pascalis R, Kashmiri SV, Schlom J, and Sabzevari H (2005) Inhibition of CD4(+)25+ T regulatory cell function implicated in enhanced immune response by low-dose cyclophosphamide. *Blood* **105**:2862–2868.

Medina-Echeverz J, Fioravanti J, Zabala M, Ardaiz N, Prieto J, and Berraondo P (2011) Successful colon cancer eradication after chemoimmunotherapy is associated with profound phenotypic change of intratumoral myeloid cells. *J Immunol* **186**:807–815.

Mkrtichyan M, Najjar YG, Raulfs EC, Abdalla MY, Samara R, Rotem-Yehudar R, Cook L, and Khleif SN (2011) Anti-PD-1 synergizes with cyclophosphamide to induce potent anti-tumor vaccine effects through novel mechanisms. *Eur J Immunol* **41**:2977–2986.

Onizuka S, Tawara I, Shimizu J, Sakaguchi S, Fujita T, and Nakayama E (1999) Tumor rejection by in vivo administration of anti-CD25 (interleukin-2 receptor α) monoclonal antibody. *Cancer Res* **59**:3128–3133.

Palucka K and Banchereau J (2012) Cancer immunotherapy via dendritic cells. *Nat Rev Cancer* **12**:265–277.

Parra-Guillen ZP, Berraondo P, Grenier E, Ribba B, and Troconiz IF (2013) Mathematical model approach to describe tumour response in mice after vaccine administration and its applicability to immune-stimulatory cytokine-based strategies. *AAPS J* **15**:797–807.

Préville X, Ladant D, Timmerman B, and Leclerc C (2005) Eradication of established tumors by vaccination with recombinant Bordetella pertussis adenylate cyclase carrying the human papillomavirus 16 E7 oncoprotein. *Cancer Res* **65**:641–649.

Rocchetti M, Simeoni M, Pesenti E, De Nicolao G, and Poggesi I (2007) Predicting the active doses in humans from animal studies: a novel approach in oncology. *Eur J Cancer* **43**:1862–1868.

Rocchetti M, Del Bene F, Germani M, Fiorentini F, Poggesi I, Pesenti E, Magni P, and De Nicolao G (2009) Testing additivity of anticancer agents in pre-clinical studies: a PK/PD modelling approach. *Eur J Cancer* **45**:3336–3346.

Rosenberg SA, Yang JC, and Restifo NP (2004) Cancer immunotherapy: moving beyond current vaccines. *Nat Med* **10**:909–915.

Rynkiewicz D, Rathkopf M, Sim I, Waytes AT, Hopkins RJ, Giri L, DeMuria D, Ransom J, Quinn J, and Nabors GS, et al. (2011) Marked enhancement of the immune response to BioThrax® (Anthrax Vaccine Adsorbed) by the TLR9 agonist CPG 7909 in healthy volunteers. *Vaccine* **29**:6313–6320.

Speiser DE, Liénard D, Rufer N, Rubio-Godoy V, Rimoldi D, Lejeune F, Krieg AM, Cerottini JC, and Romero P (2005) Rapid and strong human CD8+ T cell responses to vaccination with peptide, IFA, and CpG oligodeoxynucleotide 7909. *J Clin Invest* **115**:739–746.

Walter S, Weinschenk T, Stenzl A, Zdrojowy R, Pluzanska A, Szczylik C, Staehler M, Brugger W, Dietrich PY, and Mendrzyk R, et al. (2012) Multipeptide immune response to cancer vaccine IMA901 after single-dose cyclophosphamide associates with longer patient survival. *Nat Med* **18**:1254–1261.

Wong H, Choo EF, Alicke B, Ding X, La H, McNamara E, Theil FP, Tibbitts J, Friedman LS, and Hop CE, et al. (2012) Antitumor activity of targeted and cytotoxic agents in murine subcutaneous tumor models correlates with clinical response. *Clin Cancer Res* **18**:3846–3855.

Address correspondence to: Dr. Iñaki F. Trocóniz, Department of Pharmacy and Pharmaceutical Technology, School of Pharmacy, University of Navarra. C/Irunlarrea 1, 31008 Pamplona, Navarra, Spain. E-mail: itroconiz@unav.es